

J. Synchrotron Rad. (1999), **6**, 155–157

Rapid and sensitive XAFS using a tunable X-ray undulator

Hiroyuki Oyanagi,^a Masashi Ishii,^b Chul-Ho Lee,^a Naurang.L. Saini,^c Yuji Kuwahara,^d Akira Saito,^d Yasuo Izumi^e and Hideki Hashimoto^f

^aElectrotechnical Laboratory, 1-1-4 Umezono, Tsukuba 305-8568, Japan, ^bJASRI, Kamigori, Ako-gun, Hyogo 678-12, Japan, ^cUniversita di Roma "La Sapienza", Dipartimento di Fisica, 00185 Roma, Italy, ^dOsaka University, 2-1 Yamadaoka, Suita, Osaka 565-0871, Japan, ^eTokyo Institute of Technology, 4259 Nagatsuta, Midori-ku, Yokohama 226-8502, Japan, ^fTORAY Research Center, 337 Sonoyama, Otsu-shi 520-8567, Japan. E-mail:oyanagi@etl.go.jp

We describe the design and performance of a high-brilliance XAFS station at BL10XU of SPring-8 planned for rapid and sensitive X-ray absorption fine structure (XAFS). A deflection parameter K_y of undulator and a double crystal monochromator have been successfully tuned to cover a wide range in energy (5–30 keV). For a high throughput fluorescence data acquisition, a 100-pixel Ge detector has been developed which allows a total count rate exceeding 30 MHz with a typical energy resolution of 270 eV at 5.9 keV. A three-axis high-precision goniometer is designed to provide any polarization geometry including a grazing-incidence fluorescence excitation.

Key words: tunable undulator, pixel array detector, pump and probe XAFS

1. Introduction

Use of X-ray undulators inserted in ultra-low emittance (<10 nmrad) storage rings opened new opportunities for local structure studies beyond the limitations in concentration and/or time resolution. Rapid and sensitive XAFS is particularly powerful for in-situ studies where a sample volume or concentration is strictly limited. For example, we have demonstrated that pump and probe X-ray absorption fine structure (XAFS) (Oyanagi, Kolobov & Tanaka, 1998) can provide a snapshot information on the local lattice distortion, relaxation and bond alternation as a result of electronic excitation (Kolobov, Oyanagi & Tanaka, 1997). The observation that the average coordination in chalcogenide glasses increases during the photo-illumination at low temperature showed that the dominant photo-induced defect state is a pair of neutral C^0_3 states and not a charged defect pairs such as $C^0_3-C^0_3$ (Kolobov, Oyanagi & Tanaka, 1997). The increased average coordination number provided a direct evidence of local melting induced by photoexcitation (photomelting).

Rapid and sensitive XAFS based on a fluorescence detection mode and a tunable undulator discussed as mere feasibility (Oyanagi, 1993) is now becoming a routine tool (Rogalev, Gotte, Goulon et al., 1998). In this paper, we focus our attention on the combination of a tunable X-ray undulator and a high efficiency detector which would increase the capability of XAFS beyond the present limit. We have designed and built the high-brilliance XAFS station at the undulator beamline BL10XU, SPring-8. A novel 100-pixel array detector (PAD) as a high throughput X-ray detector has been devel-

oped and a computer control of undulator deflection parameter and a double crystal monochromator has allowed a continuous energy scan over an energy range 5–30 keV with a high energy resolution ($\Delta E/E < 2 \times 10^{-4}$).

2. Light source and beamline optics

The optics of BL10XU at SPring-8 is quite simple, i.e., major optical components are a "rotated-inclined" double crystal monochromator (Ishikawa, 1995) and a double flat mirror with a variable cut-off energy. In Fig. 1, undulator brilliance spectra for a standard in-vacuum type undulator (U032V) (Kitamura, 1994) with different deflection parameter values ($K_y = 0.3, 1.25, 2.3$) are shown. On varying an undulator gap from 9.6 mm to 22 mm, a wide energy range (5–30 keV) is covered using the first and third higher harmonics. On going to a higher energy with a smaller K_y value, the brilliance decreases while the band width increases. Since a typical energy range of ~1 keV is required as a routine EXAFS scan, both monochromator and undulator gap should be controlled during a scan; an undulator gap is varied so that a monochromator acceptance can track the undulator peak.

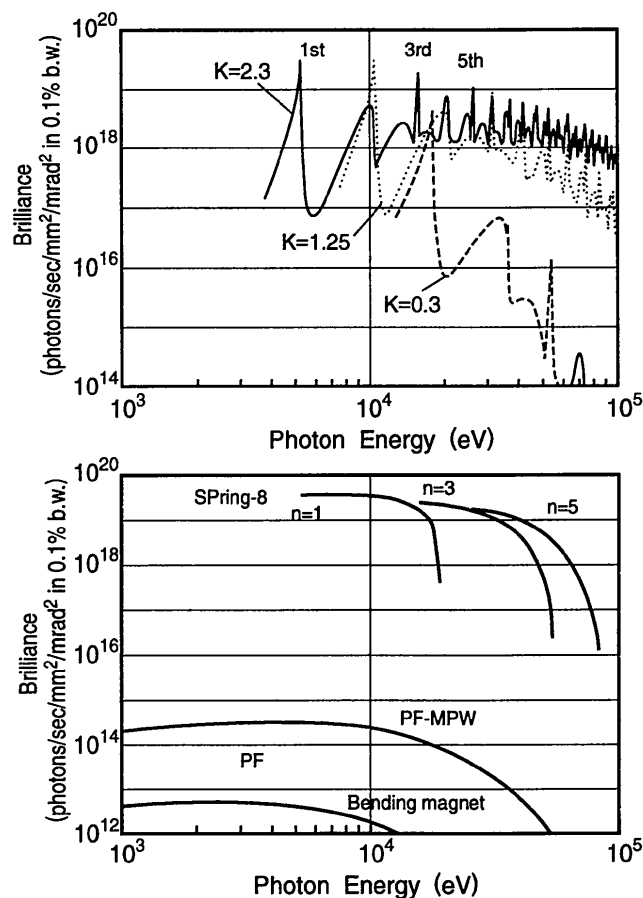


Figure 1
Brilliance of undulator for BL10XU at SPring-8 (Kitamura, 1994). Three spectra with various deflection parameter values ($K_y = 0.3, 1.25, 2.3$) are shown in logarithmic scale (upper column). Envelopes of these peaks are compared with brilliance for MPW and bending magnet at the Photon Factory (lower column).

Higher harmonics and background radiation from bending magnets are minimized by a double flat mirror with a variable critical

energy. For a lower energy range (5-16 keV), the fundamental radiation is used while for a higher energy range (16-30 keV), the third higher harmonic radiation is tuned. An undulator gap is tuned when the intensity is reduced beyond a certain limit. The criterion for tuning an undulator gap is a user-accessible parameter and one can freely choose the optimum tuning condition. As will be discussed in Sec. 4, we have confirmed that the normalization by i_0 works with upto 30% intensity change; no glitches were observed in both transmission and fluorescence spectra due to a step-like increase of incident beam intensity upon undulator tuning. For tuning the monochromator to the first higher harmonic radiation over a wide energy, the cut-off energy of mirror is varied so that the higher harmonics component is suppressed.

Owing to a grazing-incidence angle of 1° in an asymmetric double-crystal (+, -) rotated inclined configuration, the power density on the first crystal surface becomes $\sim 5 \text{ W/mm}^2$ being reduced by $1/57.3$. We find that reflectivity calculated by a dynamical theory for a Si(111) reflection becomes larger than a symmetric case by a factor of two; the full width at half maximum (FWHM) values for rocking curves are 14.9 arcsec at 8 keV for Si(111) and 2.3 arcsec at 24 keV for Si(220). However, the observed energy resolution $\Delta E/E$ given as a convolution of rocking curve width and an angular divergence multiplied by $\cot\theta_B$ was less than 2×10^{-4} because of a small angular divergence of incident beam (4.85 mrad). The results of ray tracing based on a dynamical theory predicts the maximum photon flux at 8 keV to be 10^{14} photons/sec for 100 mA.

3. Detector

As a high efficiency X-ray detector, a novel "monolithic" 100-pixel Ge array detector is to be installed. The arrangements of pixels

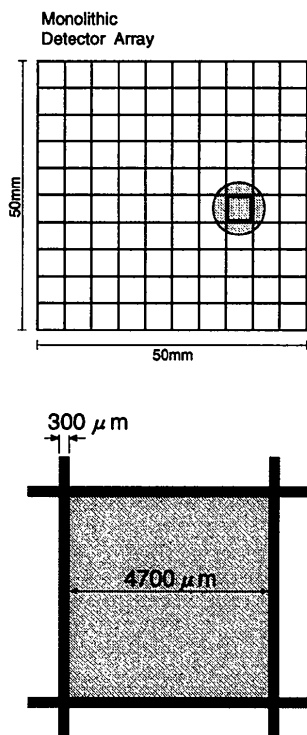


Figure 2
A monolithic Ge pixel-array detector.

are illustrated in Fig. 2. The packing ratio of a 19-element Ge detector based on a conventional technique, i.e., array of independent elements is 57% (Oyanagi, Saito & Martini, 1998). In the present design, each pixel (pure Ge) is 10 mm thick and has a dead region between pixels is ~ 0.3 mm wide, which dramatically improves the packing ratio to 88%. Each pixel has an effective area of $4.7 \text{ mm} \times 4.7 \text{ mm}$. The observed energy resolution was 212 eV at 5.9 keV at a medium count rate. This value was close to the design value expected from the pixel-ground and pixel-pixel capacitance. We estimate the energy resolution at a high count rate (3×10^5 cps) to be about 270 eV using a 1 μsec peaking time of a digital signal processor.

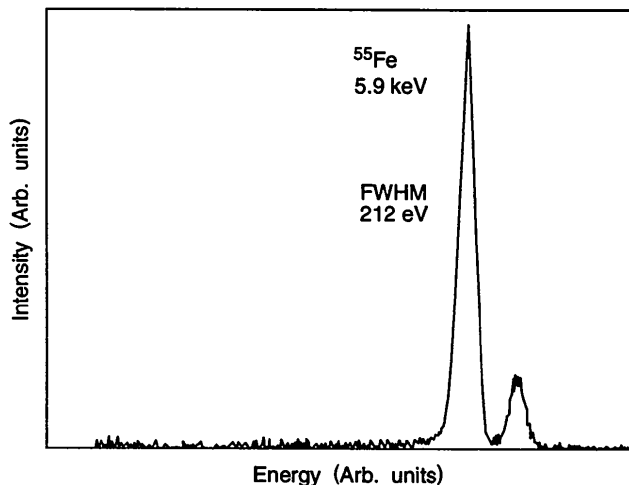


Figure 3
Energy spectrum for ^{55}Fe using one of the 100 pixels with an analog amplifier with a shaping time of 6 μsec .

Each detector pixel is equipped with PSC941 preamplifier (Penta FET). Ten FET modules are mounted on a single cooled circuit board and contacted with Ge pixels. FET circuit boards and preamplifier modules were fabricated onto separate boards which are arranged around the endcap. Performance tests for various types of Ge crystals have shown that the performance of a Ge PAD is strongly dependent on the passivation process, in contrast to a Si PAD for which SiO_2 provides a stable passivated layer. After a series of improvements, we achieved a good energy resolution (212 eV at 5.9 keV) for Ge PAD using an optimized parameters (Fig. 3). The peak-to-valley ratio in the lower energy region of ^{55}Fe peak was as high as ~ 450 .

In total, a maximum count rate of 3×10^7 cps is expected for the improved Ge PAD by optimizing the capacitance of FET. For processing the data, a commercial digital signal processors (X-ray Instrum. Assoc., DXP Model 4T) are used. For 100-channel data acquisition, twenty-five DXP modules are controlled via a CAMAC interface (WieNer, CC16) by a work station (Dell Computer, Optiplex GXMT5166) running on linux 2.1.30. Optimized parameters for operating DXP modules are downloaded so that 100-channel fluorescence data are independently recorded during a scan.

4. XAFS data acquisition

Recently, polarization-dependence in fluorescence XAFS has attracted much attention. Two topics are reviewed here. Polarized XAFS has been successfully applied to the studies of local distortions in the CuO_2 plane of high T_c superconductors (Bianconi, Saini, Lanzara et al, 1996). In these experiments, the electrical field vector should be precisely oriented to probe the radial distribution along the a-, b- and c-axis of a small single crystal with a typical dimension of 1-2 mm. For these requirements, a closed-cycle He refrigerator must have two-axis freedom of rotation, i.e., ϕ and χ -axis.

Secondly, the polarization dependence is important in surface-sensitive experiments (Oyanagi, Shioda, Kuwahara & Haga, 1995) using a grazing-incidence geometry in which vertical and horizontal sample orientations provide the information on radial distributions around an excited atom parallel and perpendicular to the surface normal, respectively. Thirdly, a grazing-incidence X-ray is used for minimizing the mismatch between probe X-ray and pump photons in "pump and probe" XAFS (Oyanagi, Kolobov & Tanaka, 1998). All these experiments require a high-precision alignment of crystal orientation. For this purpose we have designed the three-axis goniometer where a sample mounted on a closed cycle He cryostat can be oriented either vertically or horizontally and allows any orientation geometry with respect to the electrical field vector E .

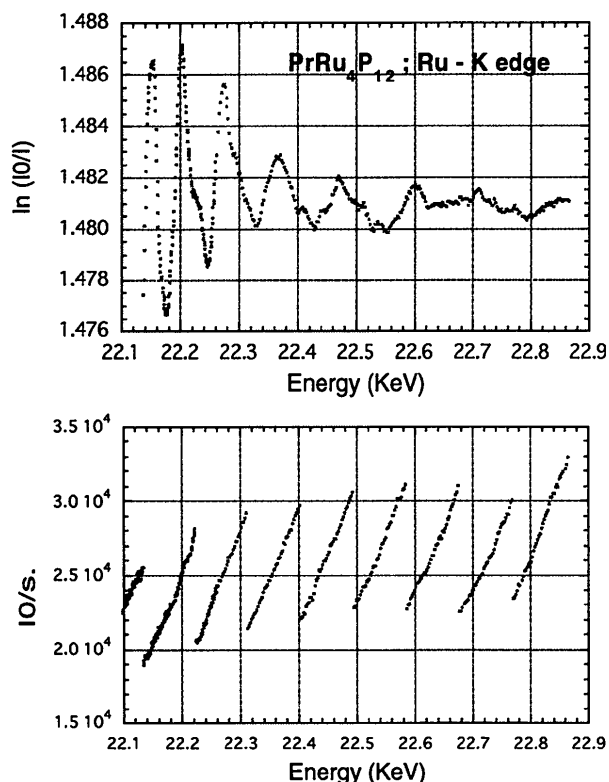


Figure 4

Ru K-edge EXAFS oscillations as a function of photon energy for $\text{PrRu}_4\text{P}_{12}$ (upper column) measured in a transmission mode and incident beam intensity (lower column).

The advantage of the present system is that one can choose the polarization geometry keeping the sample in a cryostat; e.g., one can easily switch from a horizontal orientation to a vertical one or change an azimuthal rotation angle. For a horizontal orientation, this allows one to measure the X-ray standing wave (XSW) (Oyanagi, 1998). Undulator and monochromator scanning was tested at the Ru K-edge (22.1 keV) using a powder sample of $\text{RuPr}_4\text{P}_{12}$ which shows a metal-insulator transition at 60 K. As illustrated in Fig. 4, the outputs of two ion chambers monitoring the incident and transmitted beam intensities cancel each other and no glitch was observed upon undulator tuning. The data was taken at.

5. Summary

A continuous spectroscopic scan over 1 keV and tuning over a wide energy range 5-30 keV have been achieved by controlling undulator gap at BL10XU of the SPring-8. The gap is controlled so that the intensity is within a certain limit, e.g., 30%. In spite of the degradation of crystal rocking curve due to an asymmetric reflection geometry in a rotated inclined monochromator, an energy resolution better than 2×10^{-4} was achieved. A 100-pixel pure Ge array detector has been developed for which an energy resolution of 212 eV (5.9 keV) was achieved. Our goal is to combine a high brilliance beam with a high efficiency detector in order to go beyond the present limits in concentration and/or a time-resolution. Polarization dependence for a high T_c superconductors, surface-sensitive XAFS and pump and probe experiments are possible fields of application. We put a special emphasis in the last category where dynamics in lattice distortions and relaxation would be directly measured if a data acquisition sequence is synchronized to a excitation pulse.

The authors wish to express their thanks to J. Zegenhagen for helpful suggestions regard with XSW applications, and to D. Tweet for the development of DAFS apparatus.

References

- Bianconi, A. Saini, N.L., Lanzara, A. Missori, M. Rossetti, T. Oyanagi, H. Yamaguchi, H. Oka, K. Ito, T. (1996). *Phys. Rev. Lett.* **76**, 3412-3415.
- Ishikawa, T. (1995). 5th Int. Conf. on Biophysics and Synchrotron Radiation, Grenoble.
- Kolobov, A.V., Oyanagi, H., Tanaka, K. & Tanaka, Ke. (1997). *Phys. Rev.* **B55**, 726-734.
- Kitamura, H. (1994). *Rev. Sci. Instrum.* **66**, 2007-2010.
- Oyanagi, H. (1993). *J. Appl. Phys.* **32** Suppl. 32-2, 861-865.
- Oyanagi, H. Shioda, R. Kuwahara Y. and Haga, K. (1995). *J. Synchrotron Rad.* **2**, 99-105.
- Oyanagi, H. Saito, M. Martini, M. (1998). *Nucl. Instrum. and Methods*, **A403**, 58-64.
- Oyanagi, H. (1998). *J. Synchrotron Radiation*, **5**, 48-53.
- Oyanagi, H., Kolobov, A.V. and Tanaka, K. (1998). *J. Synchrotron Radiation*, **5**, 1001-1003.
- Rogalev, A. Gotte, V. Goulon, J. Gauthier, C. Chavanne J. and Elleaume, P. (1998). *J. Synchrotron Radiation* **5**, 989-991.

(Received 10 August 1998; accepted 10 December 1998)